Journal of Sound and Vibration (2001) **247**(1), 33–57
doi:10.1006/jsvi.2001.3633, available online at http://www.idealibrary.com on IDEAL®

VISCOUS HYDROELASTIC VIBRATIONS IN A CYLINDRICAL CONTAINER WITH AN ELASTIC BOTTOM

H. F. BAUER

Institut für Raumfahrttechnik, Universität der Bundeswehr München, 85577 *Neubiberg, Germany*

AND

M. CHIBA

Department of Mechanical Engineering, Iwate University, Morioka 020-8551, *Japan.*
E-mail: mchiba@iwate-u.ac.jp

(*Received* 25 *July* 2000, *and in final form* 17 *January* 2001)

The coupled motion of a viscous liquid in a cylindrical container with an elastic bottom is treated. The liquid exhibits a free surface with surface tension. The hydroelastic frequencies and decay magnitudes are determined for the lower angular- and radial modes, for which the influences of the various parameters are investigated. A new phenomenon was detected, showing that for low liquid height ratio an aperiodic range appears, in which the viscous liquid is not able to oscillate. This range decreases with growing membrane tension and increasing mode number. In addition, it was found that higher liquid modes experience larger damping and disappear from the motion as time goes on.

1. INTRODUCTION

In modern engineering the trend towards thinner and lighter structures is predominant. This leads to a high flexibility of the system, and yields in structure–liquid systems the interaction of the elastic structure with the liquid in contact with the structure. Whether we deal with large-capacity containers for liquid storage or with propellant containers of missiles, space vehicles, satellites or space stations, the knowledge of the natural frequencies of the elastic structure and the liquid alone is no longer sufficient for the proper design of the overall vehicle and its control system. For that reason, one should know the coupled frequencies as they appear by the interaction of the oscillatory liquid *and* the elastically vibrating structure. In many cases the liquid sloshing frequencies are too close to other frequencies of the system, and result for that reason in a continuous disturbance of the motion, which in many cases leads even to instabilities and failure. A large number of analyses and experiments have been performed in recent years [1–26] for circular cylindrical containers partially filled with liquid. In all these investigations, the liquid has been considered frictionless. Damping of surface waves in an incompressible liquid has been treated for a rigid container approximately by considering the viscous dissipation in an assumed boundary layer [30]. Just recently, some studies of sloshing viscous liquid have been treated [27–34] for rigid circular cylindrical containers. In some of these studies [31, 32] the rigid container bottom conditions were satisfied, while the side wall condition could

0022-460X/01/410033 + 25 $35.00/0

only be satisfied in its normal boundary condition. These solutions are practically valid for small aspect ratios $h/a < 1$, for which the effect of the adhesion conditions of the tank bottom are predominant in comparison with sidewall adhesion contributions. For large aspect ratios $h/a > 1$, the side wall conditions are predominant and have been treated in references [33, 34] for rigid container bottom. The hydroelastic behavior of a rigid circular cylinder with a complete coverage of the liquid surface in the form of a flexible membrane or an elastic plate has been treated for viscous liquid recently [35].

Presented in what follows is an investigation of the coupled frequencies of a hydroelastic system filled with a *viscous* liquid and consisting of a circular cylindrical tank with an elastic bottom. The structure of the bottom of the container may be described by a flexible membrane or an elastic plate. The analysis is performed by solving the Stokes equations and observing only the normal side wall boundary condition. This is justified for small container filling aspect ratios $h/a < 1$, where the contribution of the bottom represents the predominant contribution to the damping behavior of the hydroelastic system.

The problem may also be treated for a container bottom described by an elastic plate with various boundary conditions. This means that the plate could be considered clamped, simply supported or guided, such that the rim of the plate would be able to move up and down the wall of the cylinder, exhibiting no shear forces. The case of elastically supported boundary, where the edge rotation would be opposed by spiral springs having a distributed stiffness K (moment per unit length), could also be treated easily.

2. MATHEMATICAL FORMULATION OF THE PROBLEM

A circular cylindrical container of diameter $2a$ is filled to a height h with an incompressible and viscous liquid of density ρ and dynamic viscosity η. The container side wall $r = a$ is considered rigid, while the container bottom is treated as an elastic member of the system, that may be either described by a flexible membrane or an elastic plate (Figure 1). The free liquid surface exhibits a surface tension σ. Assuming small displacement and small velocities, the hydroelastic system has to satisfy the Stokes equations

$$\frac{\partial u}{\partial t} + \frac{1}{\rho}\frac{\partial p}{\partial r} = \nu\left[\frac{\partial^2 u}{\partial r^2} + \frac{1}{r}\frac{\partial u}{\partial r} - \frac{u}{r^2} + \frac{1}{r^2}\frac{\partial^2 u}{\partial \varphi^2} + \frac{\partial^2 u}{\partial z^2} - \frac{2}{r^2}\frac{\partial v}{\partial \varphi}\right] \tag{1a}$$

in radial direction r,

$$\frac{\partial v}{\partial t} + \frac{1}{\rho}\frac{1}{r}\frac{\partial p}{\partial \varphi} = \nu\left[\frac{\partial^2 v}{\partial r^2} + \frac{1}{r}\frac{\partial v}{\partial r} - \frac{v}{r^2} + \frac{1}{r^2}\frac{\partial^2 v}{\partial \varphi^2} + \frac{\partial^2 v}{\partial z^2} + \frac{2}{r^2}\frac{\partial u}{\partial \varphi}\right] \tag{1b}$$

in angular direction φ, and

$$\frac{\partial w}{\partial t} + \frac{1}{\rho}\frac{\partial p}{\partial z} = \nu\left[\frac{\partial^2 w}{\partial r^2} + \frac{1}{r}\frac{\partial w}{\partial r} + \frac{1}{r^2}\frac{\partial^2 w}{\partial \varphi^2} + \frac{\partial^2 w}{\partial z^2}\right] - g \tag{1c}$$

in axial direction z. The velocity of the liquid is shown by $\mathbf{v} = u\mathbf{e}_r + v\mathbf{e}_\varphi + w\mathbf{k}$, p is the pressure distribution, g the gravity constant and $\nu = \eta/\rho$ the kinematic viscosity. In addition, the continuity equation

$$\frac{\partial u}{\partial r} + \frac{u}{r} + \frac{1}{r}\frac{\partial v}{\partial \varphi} + \frac{\partial w}{\partial z} = 0 \tag{2}$$

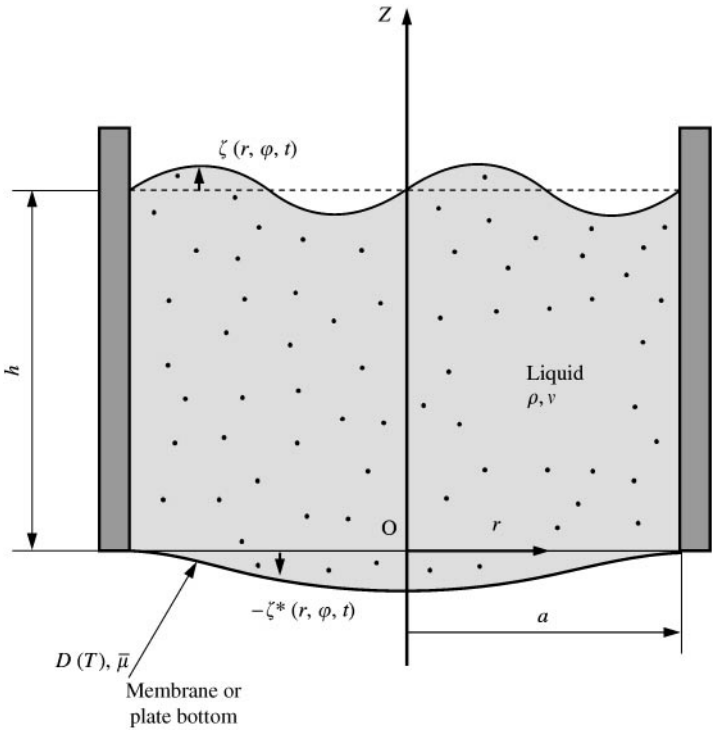

Figure 1. Cylindrical container with an elastic bottom filled with viscous liquid.

has to be satisfied. The pressure is given by

$$p(r, \varphi, z, t) = p_o - \rho g z + \bar{p}(r, \varphi, z, t) \tag{3}$$

and the free surface conditions are given by

$$\frac{\partial \zeta}{\partial t} = w \qquad \text{at } z = h \tag{4}$$

and

$$\bar{p} - 2\eta \frac{\partial w}{\partial z} + \sigma \left[\frac{\partial^2 \varsigma}{\partial r^2} + \frac{1}{r} \frac{\partial \varsigma}{\partial r} + \frac{1}{r^2} \frac{\partial^2 \varsigma}{\partial \varphi^2} - \frac{\rho g}{\sigma} \zeta \right] = const \tag{5}$$

with $\zeta(r, \varphi, t)$ as the free surface displacement at $z = h$. Kinematic condition (4) expresses the equality of the velocity of the free surface with that of a particle at the free surface, while the dynamic condition (5) is nothing but the normal shear stress relation at the free liquid surface.

The viscous liquid has to satisfy the vanishing of the normal velocity

$$u = 0 \qquad \text{at the wall} \quad r = a \tag{6}$$

and, if it is anchored at $z = h$, $r = a$, the vanishing of the motion of the contact line:

$$\zeta = 0 \qquad \text{at } r = a. \tag{7}$$

Actually, the plate exhibits a displacement ξ^* in r direction, η^* in φ direction and ζ^* in z direction, which would be described by coupled differential equations and three additional compatibility conditions, i.e., $\partial\xi^*/\partial t = u$; $\partial\eta^*/\partial t = v$ and $\partial\xi^*/\partial t = w$ at $z = 0$. Assuming, however, that the radial-(ξ^*) and angular-(η^*) displacements of the plate are small compared to that in axial direction ζ^* yields the compatibility equations (15) and (16). Since the liquid contact line is considered to be anchored at the wall, the adherence conditions $v = w = 0$ at $r = a$ are abandoned for that weaker condition of anchored contact line at $r = a$, i.e., equation (7).

If the bottom is considered as a membrane, then it will have to satisfy the membrane equation

$$T\left[\frac{\partial^2\varsigma^*}{\partial r^2} + \frac{1}{r}\frac{\partial\varsigma^*}{\partial r} + \frac{1}{r^2}\frac{\partial^2\varsigma^*}{\partial\varphi^2}\right] = \mu\frac{\partial^2\varsigma^*}{\partial t^2} + \rho g\zeta^* - \left(\bar{p} - 2\eta\frac{\partial w}{\partial z}\right)_{z=0} \tag{8}$$

with the boundary condition

$$\zeta^* = 0 \qquad \text{at } r = a \tag{9}$$

where $\zeta^*(r, \varphi, t)$ is the displacement of the membrane, T the tension of the membrane and μ its mass per unit area. If the tank bottom is considered an elastic plate, it has to satisfy

$$D\left[\frac{\partial^2}{\partial r^2} + \frac{1}{r}\frac{\partial}{\partial r} + \frac{1}{r^2}\frac{\partial^2}{\partial\varphi^2}\right]^2\varsigma^* + \mu\frac{\partial^2\varsigma^*}{\partial t^2} = -\rho g\zeta^* + \left(\bar{p} - 2\eta\frac{\partial w}{\partial z}\right)_{z=0}, \tag{10}$$

where $D = E\delta^{*3}/12(1 - \bar{\nu}^2)$ is the flexural rigidity of the plate, δ^* its thickness, $\bar{\nu}$ the Poisson ratio and E Young's modulus of elasticity. In the analysis, damping of an elastic bottom is assumed to be negligibly small in comparison with that of the viscous liquid. Equation (10) has to satisfy the boundary condition for the cases of a

(a) clamped: $$\zeta^* = 0 \quad \text{and} \quad \frac{\partial\zeta^*}{\partial r} = 0 \qquad \text{at } r = a, \tag{11}$$

(b) simply supported: $$\zeta^* = 0 \quad \text{and} \quad M_r = 0 \qquad \text{at } r = a, \tag{12}$$

(c) free: $$M_r = 0 \quad \text{and} \quad V_r = 0 \qquad \text{at } r = a, \tag{13}$$

or

(d) guided: $$\frac{\partial\zeta^*}{\partial r} = 0 \quad \text{and} \quad V_r = 0 \qquad \text{at } r = a \tag{14}$$

plate, together with the compatibility conditions

$$u = v = 0 \qquad \text{at } z = 0. \tag{15}$$

and (not allowing any cavitation)

$$\frac{\partial\zeta^*}{\partial t} = w \qquad \text{at } z = 0. \tag{16}$$

In these equations

$$M_r = -D\left[\frac{\partial^2\zeta^*}{\partial r^2} + \bar{\nu}\left(\frac{1}{r}\frac{\partial\zeta^*}{\partial r} + \frac{1}{r^2}\frac{\partial^2\zeta^*}{\partial\varphi^2}\right)\right] \text{ and}$$

$$V_r = -D\frac{\partial}{\partial r}\left\{\frac{\partial^2\zeta^*}{\partial r^2} + \frac{1}{r}\frac{\partial\zeta^*}{\partial r} + \frac{1}{r^2}\frac{\partial^2\zeta^*}{\partial\varphi^2}\right\} - \frac{D}{r}(1-\bar{\nu})\frac{\partial}{\partial r}\left(\frac{1}{r}\frac{\partial^2\zeta^*}{\partial\varphi^2}\right)$$

representing the bending moment and the Kelvin–Kirchhoff edge reactions of the plate.

3. METHOD OF SOLUTION

Assuming u, v, w and $\bar{p}$ proportional to $e^{im\varphi}e^{st}$, we obtain with $u(r, \varphi, z, t) = e^{st}\sum_m U_m(r, z)e^{im\varphi}$ etc., and from the Stokes equation (1) with

$$\phi = U + iV \quad \text{and} \quad \psi = U - iV \tag{17a}$$

i.e.,

$$U = \frac{1}{2}(\phi + \psi) \quad \text{and} \quad V = \frac{i}{2}(\psi - \phi) \tag{17b}$$

the partial differential equations

$$\frac{\partial^2\phi}{\partial r^2} + \frac{1}{r}\frac{\partial\phi}{\partial r} - \frac{(m+1)^2}{r^2}\phi - \frac{s}{\nu}\phi + \frac{\partial^2\phi}{\partial z^2} = \frac{1}{\eta}\left[\frac{\partial\bar{P}}{\partial r} - \frac{m}{r}\bar{P}\right], \tag{18}$$

$$\frac{\partial^2\psi}{\partial r^2} + \frac{1}{r}\frac{\partial\psi}{\partial r} - \frac{(m-1)^2}{r^2}\psi - \frac{s}{\nu}\psi + \frac{\partial^2\psi}{\partial z^2} = \frac{1}{\eta}\left[\frac{\partial\bar{P}}{\partial r} + \frac{m}{r}\bar{P}\right], \tag{19}$$

$$\frac{\partial^2 W}{\partial r^2} + \frac{1}{r}\frac{\partial W}{\partial r} - \frac{m^2}{r^2}W - \frac{s}{\nu}W + \frac{\partial^2 W}{\partial z^2} = \frac{1}{\eta}\frac{\partial\bar{P}}{\partial z} \tag{20}$$

and from the continuity equation (2)

$$\frac{\partial\phi}{\partial r} + \frac{(m+1)}{r}\phi + \frac{\partial\psi}{\partial r} - \frac{(m-1)}{r}\psi = -2\frac{\partial W}{\partial z}. \tag{21}$$

For the solution of these coupled partial differential equations, satisfying the rigid wall condition (6) we apply

$$\begin{aligned}
\phi(r, z) &= \bar{A}_{mn}(z)\mathrm{J}_{m+1}\left(\varepsilon_{mn}\frac{r}{a}\right),\\
\psi(r, z) &= -\bar{A}_{mn}(z)\mathrm{J}_{m-1}\left(\varepsilon_{mn}\frac{r}{a}\right),\\
W(r, z) &= \bar{C}_{mn}(z)\mathrm{J}_m\left(\varepsilon_{mn}\frac{r}{a}\right),\\
\bar{P}(r, z) &= \bar{D}_{mn}(z)\mathrm{J}_m\left(\varepsilon_{mn}\frac{r}{a}\right),
\end{aligned} \tag{22}$$

where ε_{mn} are the roots of $J'_m(\varepsilon) = 0$. This system of differential equations is then reduced to

$\left(\frac{d}{dz} \equiv '\right)$

$$\bar{A}''_{mn} - \mu^2_{mn}\bar{A}_{mn} = -\frac{\varepsilon_{mn}}{a\eta}\bar{D}_{mn},$$

$$\bar{C}''_{mn} - \mu^2_{mn}\bar{C}_{mn} = \frac{\bar{D}'_{mn}}{\eta}, \tag{23}$$

$$\frac{\varepsilon_{mn}}{a}\bar{A}_{mn} + \bar{C}'_{mn} = 0,$$

where $\mu^2_{mn} = \frac{\varepsilon^2_{mn}}{a^2} + \frac{s}{v}$, and renders the solution

$$\bar{A}_{mn}(z) = A_{mn}\cosh\left(\varepsilon_{mn}\frac{z}{a}\right) + B_{mn}\sinh\left(\varepsilon_{mn}\frac{z}{a}\right) + C_{mn}\cosh(\mu_{mn}z) + D_{mn}\sinh(\mu_{mn}z), \tag{24a}$$

$$\bar{C}_{mn}(z) = -\left[A_{mn}\sinh\left(\varepsilon_{mn}\frac{z}{a}\right) + B_{mn}\cosh\left(\varepsilon_{mn}\frac{z}{a}\right) + \frac{\varepsilon_{mn}}{\bar{\mu}_{mn}}\left\{C_{mn}\sinh\left(\bar{\mu}_{mn}\frac{z}{a}\right) + D_{mn}\cosh\left(\bar{\mu}_{mn}\frac{z}{a}\right)\right\}\right] \tag{24b}$$

and

$$\bar{D}_{mn}(z) = \frac{\rho s a}{\varepsilon_{mn}}\left[A_{mn}\cosh\left(\varepsilon_{mn}\frac{z}{a}\right) + B_{mn}\sinh\left(\varepsilon_{mn}\frac{z}{a}\right)\right]. \tag{24c}$$

With the free surface displacement

$$\zeta(r, \varphi, t) = e^{st}\sum_{m=0}^{\infty}\zeta_m(r)e^{im\varphi} = e^{st}\sum_{m=0}^{\infty}\sum_{n=1}^{\infty}\zeta_{mn}J_m\left(\varepsilon_{mn}\frac{r}{a}\right)e^{im\varphi} \tag{25}$$

the kinematic condition (4) yields

$$\zeta_{mn} = -\frac{1}{S}\left[\tilde{A}_{mn}\sinh\left(\varepsilon_{mn}\frac{h}{a}\right) + \tilde{B}_{mn}\cosh\left(\varepsilon_{mn}\frac{h}{a}\right) + \frac{\varepsilon_{mn}}{\bar{\mu}_{mn}}\left\{\tilde{C}_{mn}\sinh\left(\bar{\mu}_{mn}\frac{h}{a}\right) + \tilde{D}_{mn}\cosh\left(\bar{\mu}_{mn}\frac{h}{a}\right)\right\}\right] \tag{26}$$

where $S \equiv \frac{sa^2}{v}$, $\bar{\mu}^2_{mn} = \varepsilon^2_{mn} + S$ and $\tilde{A}_{mn} \equiv A_{mn}\frac{a^2}{v}$, etc.

The dynamic free surface condition (5) yields with equation (25) and the above results

$$\frac{d^2\zeta_m}{dr^2} + \frac{1}{r}\frac{d\zeta_m}{dr} - \frac{m^2}{r^2}\zeta_m - \frac{\rho g}{\sigma}\zeta_m$$

$$= -\sum_{n=1}^{\infty}\frac{\rho s a}{\sigma\varepsilon_{mn}}\left[A_{mn}\cosh\left(\varepsilon_{mn}\frac{h}{a}\right) + B_{mn}\sinh\left(\varepsilon_{mn}\frac{h}{a}\right)\right]J_m\left(\varepsilon_{mn}\frac{r}{a}\right)$$

$$-\frac{2\eta}{\sigma a}\sum_{n=1}^{\infty}\varepsilon_{mn}\left[\mathrm{A}_{mn}\cosh\left(\varepsilon_{mn}\frac{h}{a}\right)+B_{mn}\sinh\left(\varepsilon_{mn}\frac{h}{a}\right)+C_{mn}\cosh\left(\bar{\mu}_{mn}\frac{h}{a}\right)\right.$$

$$\left.+D_{mn}\sinh\left(\bar{\mu}_{mn}\frac{h}{a}\right)\right]\mathrm{J}_m\left(\varepsilon_{mn}\frac{r}{a}\right) \tag{27}$$

which exhibits the solution (for $m\neq 0$) with $\alpha^2\equiv\dfrac{\rho g a^2}{\sigma}\equiv\dfrac{g^*}{\sigma^*}$, $g^*\equiv\dfrac{ga^3}{\nu^2}$, $\sigma^*\equiv\dfrac{\sigma a}{\rho\nu^2}$,

$$\zeta_m(r)=\bar{A}_m\mathrm{I}_m\left(\alpha\frac{r}{a}\right)+\frac{S}{\sigma^*}\sum_{n=1}^{\infty}\frac{\mathrm{J}_m(\varepsilon_{mn}\,r/a)}{\varepsilon_{mn}(\varepsilon_{mn}^2+\alpha^2)}\left[\tilde{A}_{mn}\cosh\left(\varepsilon_{mn}\frac{h}{a}\right)+\tilde{B}_{mn}\sinh\left(\varepsilon_{mn}\frac{h}{a}\right)\right]$$

$$+\frac{2}{\sigma^*}\sum_{n=1}^{\infty}\frac{\varepsilon_{mn}}{\varepsilon_{mn}^2+\alpha^2}\mathrm{J}_m\left(\varepsilon_{mn}\frac{r}{a}\right)\left[\tilde{A}_{mn}\cosh\left(\varepsilon_{mn}\frac{h}{a}\right)+\tilde{B}_{mn}\sinh\left(\varepsilon_{mn}\frac{h}{a}\right)\right.$$

$$\left.+\tilde{C}_{mn}\cosh\left(\bar{\mu}_{mn}\frac{h}{a}\right)+\tilde{D}_{mn}\sinh\left(\bar{\mu}_{mn}\frac{h}{a}\right)\right]. \tag{28}$$

The anchored edge condition (7) at $r=a$ yields

$$\bar{A}_m\mathrm{I}_m(\alpha)+\frac{S}{\sigma^*}\sum_{n=1}^{\infty}\frac{\mathrm{J}_m(\varepsilon_{mn})}{\varepsilon_{mn}(\varepsilon_{mn}^2+\alpha^2)}\left[\tilde{A}_{mn}\cosh\left(\varepsilon_{mn}\frac{h}{a}\right)+\tilde{B}_{mn}\sinh\left(\varepsilon_{mn}\frac{h}{a}\right)\right]$$

$$+\frac{2}{\sigma^*}\sum_{n=1}^{\infty}\frac{\varepsilon_{mn}}{\varepsilon_{mn}^2+\alpha^2}\mathrm{J}_m(\varepsilon_{mn})\left[\tilde{A}_{mn}\cosh\left(\varepsilon_{mn}\frac{h}{a}\right)+\tilde{B}_{mn}\sinh\left(\varepsilon_{mn}\frac{h}{a}\right)\right.$$

$$\left.+\tilde{C}_{mn}\cosh\left(\bar{\mu}_{mn}\frac{h}{a}\right)+\tilde{D}_{mn}\sinh\left(\bar{\mu}_{mn}\frac{h}{a}\right)\right]=0. \tag{29}$$

Expanding $\mathrm{I}_m(\alpha r/a)$ as Dini-Series in the form [38]

$$\mathrm{I}_m\left(\alpha\frac{r}{a}\right)=2\alpha\sum_{n=1}^{\infty}\frac{\varepsilon_{mn}^2\mathrm{I}'_m(\alpha)\mathrm{J}_m(\varepsilon_{mn}\,r/a)}{\mathrm{J}_m(\varepsilon_{mn})(\varepsilon_{mn}^2+\alpha^2)(\varepsilon_{mn}^2-m^2)},$$

introducing it into equation (28), and comparing it with the results of the kinematic condition (25) and (26) yields ($n=1, 2, \ldots$)

$$2\alpha\bar{A}_m\frac{\varepsilon_{mn}^2\mathrm{I}'_m(\alpha)}{(\varepsilon_{mn}^2-m^2)\mathrm{J}_m(\varepsilon_{mn})}+\frac{S}{\sigma^*\varepsilon_{mn}}\left[\tilde{A}_{mn}\cosh\left(\varepsilon_{mn}\frac{h}{a}\right)+\tilde{B}_{mn}\sinh\left(\varepsilon_{mn}\frac{h}{a}\right)\right]$$

$$+\frac{2}{\sigma^*}\varepsilon_{mn}\left[\tilde{A}_{mn}\cosh\left(\varepsilon_{mn}\frac{h}{a}\right)+\tilde{B}_{mn}\sinh\left(\varepsilon_{mn}\frac{h}{a}\right)\right.$$

$$\left.+\tilde{C}_{mn}\cosh\left(\bar{\mu}_{mn}\frac{h}{a}\right)+\tilde{D}_{mn}\sinh\left(\bar{\mu}_{mn}\frac{h}{a}\right)\right]$$

$$+\frac{\varepsilon_{mn}^2+\alpha^2}{S}\left[\tilde{A}_{mn}\sinh\left(\varepsilon_{mn}\frac{h}{a}\right)+\tilde{B}_{mn}\cosh\left(\varepsilon_{mn}\frac{h}{a}\right)\right.$$

$$\left.+\frac{\varepsilon_{mn}}{\bar{\mu}_{mn}}\left\{\tilde{C}_{mn}\sinh\left(\bar{\mu}_{mn}\frac{h}{a}\right)+\tilde{D}_{mn}\cosh\left(\bar{\mu}_{mn}\frac{h}{a}\right)\right\}\right]=0. \tag{30}$$

For axisymmetric vibration with $m=0$, equation (28) exhibits an additional term P_o^*. The expansion of $\mathrm{I}_o(\alpha r/a)$ into Dini-Series yields

$$\mathrm{I}_o\left(\alpha\frac{r}{a}\right)=\frac{2}{\alpha}\mathrm{I}_1(\alpha)+2\alpha\sum_{n=1}^{\infty}\frac{\mathrm{I}_1(\alpha)\,\mathrm{J}_o(\varepsilon_{on}\,r/a)}{\mathrm{J}_o(\varepsilon_{on})(\varepsilon_{on}^2+\alpha^2)}$$

and from equation (28) for $m=0$, and the comparison of it with the results of the kinematic condition, we obtain the equations

$$\frac{2}{\alpha}\mathrm{I}_1(\alpha)\bar{A}_o+P_o^*=0 \tag{31}$$

and

$$2\alpha\frac{\mathrm{I}_1(\alpha)}{\mathrm{J}_o(\varepsilon_{on})}\bar{A}_o+\frac{S}{\sigma^*\varepsilon_{on}}\left[\tilde{A}_{on}\cosh\left(\varepsilon_{on}\frac{h}{a}\right)+\tilde{B}_{on}\sinh\left(\varepsilon_{on}\frac{h}{a}\right)\right]$$

$$+\frac{2}{\sigma^*}\varepsilon_{on}\left[\tilde{A}_{on}\cosh\left(\varepsilon_{on}\frac{h}{a}\right)+\tilde{B}_{on}\sinh\left(\varepsilon_{on}\frac{h}{a}\right)+\tilde{C}_{on}\cosh\left(\bar{\mu}_{on}\frac{h}{a}\right)+\tilde{D}_{on}\sinh\left(\bar{\mu}_{on}\frac{h}{a}\right)\right]$$

$$+\frac{\varepsilon_{on}^2+\alpha^2}{S}\left[\tilde{A}_{on}\sinh\left(\varepsilon_{on}\frac{h}{a}\right)+\tilde{B}_{on}\cosh\left(\varepsilon_{on}\frac{h}{a}\right)\right.$$

$$\left.+\frac{\varepsilon_{on}}{\bar{\mu}_{on}}\left\{\tilde{C}_{on}\sinh\left(\bar{\mu}_{on}\frac{h}{a}\right)+\tilde{D}_{on}\cosh\left(\bar{\mu}_{on}\frac{h}{a}\right)\right\}\right]=0. \tag{32}$$

for $n=1, 2, \ldots$

3.1. MEMBRANE BOTTOM

If the bottom is treated as a membrane, equation (8) has to be solved with the boundary condition (9) and

$$\zeta^*(r,\varphi,t)=\mathrm{e}^{st}\sum_{m=0}^{\infty}\zeta_m^*(r)\mathrm{e}^{\mathrm{i}m\varphi}=\mathrm{e}^{st}\sum_{m=0}^{\infty}\sum_{n=1}^{\infty}\zeta_{mn}^*\,\mathrm{J}_m\left(\varepsilon_{mn}\frac{r}{a}\right)\mathrm{e}^{\mathrm{i}m\varphi}. \tag{33}$$

We obtain with the compatibility condition (16)

$$\zeta_{mn}^{*} = -\frac{1}{S}\left[\tilde{B}_{mn} + \frac{\varepsilon_{mn}}{\bar{\mu}_{mn}}\tilde{D}_{mn}\right] \tag{34}$$

the ordinary differential equation

$$\frac{\mathrm{d}^2\zeta_m^*}{\mathrm{d}r^2} + \frac{1}{r}\frac{\mathrm{d}\zeta_m^*}{\mathrm{d}r} - \frac{m^2}{r^2}\zeta_m^* - \frac{\mu s^2 + \rho g}{T}\zeta_m^*$$

$$= -\sum_{n=1}^{\infty}\frac{\rho s a}{\varepsilon_{mn} T} A_{mn}\mathrm{J}_m\left(\varepsilon_{mn}\frac{r}{a}\right) - \frac{2\eta}{Ta}\sum_{n=1}^{\infty}\varepsilon_{mn}\mathrm{J}_m\left(\varepsilon_{mn}\frac{r}{a}\right)(A_{mn} + C_{mn}). \tag{35}$$

From the compatibility condition (15) we obtain

$$\tilde{A}_{mn} + \tilde{C}_{mn} = 0 \tag{36}$$

for $n = 1, 2, 3, \ldots$
and therefore the solution of the inhomogeneous ordinary differential equation (35) is given by

$$\zeta_m^*(r) = \bar{B}_m \mathrm{I}_m\left(\beta\frac{r}{a}\right) + \frac{S}{T^*}\sum_{n=1}^{\infty}\frac{\tilde{A}_{mn}\mathrm{J}_m(\varepsilon_{mn}\, r/a)}{\varepsilon_{mn}(\varepsilon_{mn}^2 + \beta^2)}, \tag{37}$$

where $T^* \equiv \dfrac{Ta}{\rho v^2}$ and $\beta^2 \equiv \dfrac{\mu s^2 a^2 + \rho g a^2}{T} \equiv \dfrac{\mu^* S^2 + g^*}{T^*}$ with $\mu^* \equiv \dfrac{\mu}{\rho a}$ and $g^* \equiv g\dfrac{a^3}{v^2}$. The boundary condition (9) at $r = a$ yields

$$\bar{B}_m \mathrm{I}_m(\beta) + \frac{S}{T^*}\sum_{n=1}^{\infty}\frac{\tilde{A}_{mn}\mathrm{J}_m(\varepsilon_{mn})}{\varepsilon_{mn}[\varepsilon_{mn}^2 + \beta^2]} = 0. \tag{38}$$

After expanding $\mathrm{I}_m(\beta r/a)$ into a Dini-Series, introducing it into equation (37) and comparing coefficients with ζ^* from the compatibility condition (16), results in

$$2\beta\,\bar{B}_m\frac{\varepsilon_{mn}^2\mathrm{I}'_m(\beta)}{\mathrm{J}_{mn}(\varepsilon_{mn})(\varepsilon_{mn}^2 - m^2)} + \frac{S}{T^*\varepsilon_{mn}}\tilde{A}_{mn} + \frac{(\varepsilon_{mn}^2 + \beta^2)}{S}\left[\tilde{B}_{mn} + \frac{\varepsilon_{mn}}{\bar{\mu}_{mn}}\tilde{D}_{mn}\right] = 0 \tag{39}$$

for $m \neq 0$, $n = 1, 2, \ldots$

Equations (39), (38), (36), (29) and (30) form together with the vanishing shear stress condition and the free surface, i.e.,

$$\tau_{rz} = 0 \quad \text{and} \quad \tau_{\varphi z} = 0 \qquad \text{at } z = h \tag{40}$$

which results in

$$2\varepsilon_{mn}\left[\tilde{A}_{mn}\sinh\left(\varepsilon_{mn}\frac{h}{a}\right) + \tilde{B}_{mn}\cosh\left(\varepsilon_{mn}\frac{h}{a}\right)\right]\sqrt{\varepsilon_{mn}^2 + S}$$

$$+ (2\varepsilon_{mn}^2 + S)\left[\tilde{C}_{mn}\sinh\left(\bar{\mu}_{mn}\frac{h}{a}\right) + \tilde{D}_{mn}\cosh\left(\bar{\mu}_{mn}\frac{h}{a}\right)\right] = 0 \tag{41}$$

for $n = 1, 2, \ldots,$
a system of $(4n + 2)$ linear homogeneous equations for $\tilde{A}_{mn}$, $\tilde{B}_{mn}$, $\tilde{C}_{mn}$, $\tilde{D}_{mn}$, $\bar{A}_m$, *and* $\bar{B}_m$ of which the vanishing coefficient determinant represents the frequency equation for the coupled hydroelastic system.

For *axisymmetric* motion $m = 0$, the expansion of $\mathrm{I}_o\left(\beta \dfrac{r}{a}\right)$ into a Dini-Series results in

$$\mathrm{I}_o\left(\beta \frac{r}{a}\right) = \frac{2}{\beta}\mathrm{I}_1(\beta) + 2\beta \sum_{n=1}^{\infty} \frac{\mathrm{I}_1(\beta)\mathrm{J}_o(\varepsilon_{on}\, r/a)}{\mathrm{J}_o(\varepsilon_{on})(\varepsilon_{on}^2 + \beta^2)}.$$

In the solution of equation (33) for $m = 0$, a constant $\bar{P}_o$ appears and we obtain from the same expansion procedure by comparison

$$\frac{2}{\beta}\mathrm{I}_1(\beta)\bar{B}_o + \bar{P}_o = 0 \tag{42}$$

and

$$2\beta \frac{\mathrm{I}_1(\beta)}{\mathrm{J}_o(\varepsilon_{on})}\bar{B}_o + \frac{S}{T^*\varepsilon_{on}}\tilde{A}_{on} + \frac{(\varepsilon_{on}^2 + \beta^2)}{S}\left[\tilde{B}_{on} + \frac{\varepsilon_{on}}{\sqrt{\varepsilon_{on}^2 + S}}\tilde{D}_{on}\right] = 0 \tag{43}$$

for $n = 1, 2, \ldots$.
The vanishing determinant of equations (43), (42) and those equations for $m = 0$ like equations (41), (36), (38) with the additional term $\bar{P}_o$ and equations (29), (31) and (32) represent the frequency equation for the axisymmetric case $m = 0$. They are $(4n + 4)$ linear homogeneous equations in $\tilde{A}_{on}$, $\tilde{B}_{on}$, $\tilde{C}_{on}$, $\tilde{D}_{on}$ and $\bar{A}_o$, $\bar{B}_o$, P_o^*, $\bar{P}_o$.

3.2. PLATE BOTTOM

If the bottom is treated as an elastic plate, equation (10) has to be solved with one of the boundary condition sets (11)–(14) together with the compatibility condition (16). It is with equation (33) and $\tilde{\zeta}_m^* \equiv \varsigma_m^*(r)$ for the plate

$$\left(\frac{\mathrm{d}^2}{\mathrm{d}r^2} + \frac{1}{r}\frac{\mathrm{d}}{\mathrm{d}r} - \frac{m^2}{r^2}\right)^2 \tilde{\zeta}_m^* + \left(\frac{\mu^* S^2 + g^*}{D^* a^4}\right)\tilde{\zeta}_m^* = \frac{S}{a^4 D^*}\sum_{n=1}^{\infty}\frac{\tilde{A}_{mn}}{\varepsilon_{mn}}\mathrm{J}_m\left(\varepsilon_{mn}\frac{r}{a}\right) \tag{44}$$

which exhibits the solution

$$\tilde{\zeta}_m^*(r) = \bar{C}_m \mathrm{I}_m\left(\gamma \frac{r}{a}\right) + \bar{D}_m \mathrm{J}_m\left(\gamma \frac{r}{a}\right) + \frac{S}{D^*}\sum_{n=1}^{\infty}\frac{\tilde{A}_{mn}\mathrm{J}_m(\varepsilon_{mn}\, r/a)}{\varepsilon_{mn}(\varepsilon_{mn}^4 - \gamma^4)} \tag{45}$$

where $\beta^{*4} = \dfrac{\mu^* S^2 + g^*}{D^*}$, $\gamma \equiv \sqrt{\mathrm{i}}\beta^*$ and $D^* \equiv \dfrac{D}{\rho v^2 a}$.

3.2.1. *Clamped plate*

For a clamped plate, the boundary conditions (11) have to be satisfied, yielding

$$\bar{C}_m \mathrm{I}_m(\gamma) + \bar{D}_m \mathrm{J}_m(\gamma) + \frac{S}{D^*}\sum_{n=1}^{\infty}\frac{\tilde{A}_{mn}\mathrm{J}_m(\varepsilon_{mn})}{\varepsilon_{mn}(\varepsilon_{mn}^4 - \gamma^4)} = 0 \tag{46a}$$

and

$$\bar{C}_m \mathrm{I}'_m(\gamma) + \bar{D}_m \mathrm{J}'_m(\gamma) = 0. \tag{46b}$$

After expansion of $\mathrm{I}_m\left(\gamma \frac{r}{a}\right)$ and $\mathrm{J}_m\left(\gamma \frac{r}{a}\right)$ into Dini-Series, i.e.,

$$\mathrm{I}_m\left(\gamma \frac{r}{a}\right) = 2\gamma \sum_{n=1}^{\infty} \frac{\varepsilon_{mn}^2 \mathrm{I}'_m(\gamma)\mathrm{J}_m(\varepsilon_{mn}\, r/a)}{\mathrm{J}_m(\varepsilon_{mn})(\varepsilon_{mn}^2 + \gamma^2)(\varepsilon_{mn}^2 - m^2)}$$

and

$$\mathrm{J}_m\left(\gamma \frac{r}{a}\right) = 2\gamma \sum_{n=1}^{\infty} \frac{\varepsilon_{mn}^2 \mathrm{J}'_m(\gamma)\mathrm{J}_m(\varepsilon_{mn}\, r/a)}{\mathrm{J}_m(\varepsilon_{mn})(\varepsilon_{mn}^2 - \gamma^2)(\varepsilon_{mn}^2 - m^2)}$$

introducing them into equation (45) and comparing it with the result of the compatibility condition (16) yields

$$2\gamma \bar{C}_m \frac{\varepsilon_{mn}^2 \mathrm{I}'_m(\gamma)}{(\varepsilon_{mn}^2 + \gamma^2)} + 2\gamma \bar{D}_m \frac{\varepsilon_{mn}^2 \mathrm{J}'_m(\gamma)}{(\varepsilon_{mn}^2 - \gamma^2)} + \frac{S\tilde{A}_{mn}\mathrm{J}_{mn}(\varepsilon_{mn})(\varepsilon_{mn}^2 - m^2)}{D^*\varepsilon_{mn}(\varepsilon_{mn}^4 - \gamma^4)}$$

$$+ \frac{(\varepsilon_{mn}^2 - m^2)\mathrm{J}_{mn}(\varepsilon_{mn})}{S}\left[\tilde{B}_{mn} + \frac{\varepsilon_{mn}}{\sqrt{\varepsilon_{mn}^2 + S}}\tilde{D}_{mn}\right] = 0 \tag{47}$$

for $n = 1, 2, \ldots$. The vanishing coefficient determinant of equations (46a), (46b), (47), (36), (41), (29) and (30) is of order $(4n + 3)$ and represents the frequency equation for the hydroelastic system ($m \neq 0$) with a plate bottom.

If the system performs *axisymmetric* oscillations $m = 0$, the elastic plate equation yields the inhomogeneous and ordinary differential equation

$$\left[\frac{\mathrm{d}^2}{\mathrm{d}r^2} + \frac{1}{r}\frac{\mathrm{d}}{\mathrm{d}r}\right]^2 \tilde{\zeta}_o^* + \left[\frac{\mu^* S^2 + g^*}{D^* a^4}\right]\tilde{\zeta}_o^* = \frac{S}{D^* a^4} \sum_{n=1}^{\infty} \frac{\mathrm{J}_o(\varepsilon_{mn}\, r/a)}{\varepsilon_{mn}} \tilde{A}_{on} + P_o \tag{48}$$

which exhibits the solution

$$\tilde{\zeta}_o^*(r) = \bar{C}_o \mathrm{I}_o\left(\gamma \frac{r}{a}\right) + \bar{D}_o \mathrm{J}_o\left(\gamma \frac{r}{a}\right) + \frac{S}{D^*} \sum_{n=1}^{\infty} \frac{\tilde{A}_{on}\, \mathrm{J}_o(\varepsilon_{on}\, r/a)}{\varepsilon_{mn}(\varepsilon_{on}^4 - \gamma^4)} + P_o^*. \tag{49}$$

The clamped-in conditions yield the two equations

$$\mathrm{I}_o(\gamma)\bar{C}_o + \mathrm{J}_o(\gamma)\bar{D}_o + \frac{S}{D^*} \sum_{n=1}^{\infty} \frac{\mathrm{J}_o(\varepsilon_{on})}{\varepsilon_{on}(\varepsilon_{on}^4 - \gamma^4)} \tilde{A}_{on} + P_o^* = 0, \tag{50a}$$

$$\mathrm{I}_1(\gamma)\bar{C}_o - \mathrm{J}_1(\gamma)\bar{D}_o = 0. \tag{50b}$$

Expanding $\mathrm{I}_o\left(\gamma \frac{r}{a}\right)$ and $\mathrm{J}_o\left(\gamma \frac{r}{a}\right)$, introducing them into equation (49) and comparing with the results of the compatibility condition (16) yields

$$2\bar{C}_o \mathrm{I}_1(\gamma) + 2\bar{D}_o \mathrm{J}_1(\gamma) + \gamma P_o^* = 0 \tag{51a}$$

and

$$2\gamma \frac{\mathrm{I}_1(\gamma)}{(\varepsilon_{on}^2 + \gamma^2)} \bar{C}_o + 2\gamma \frac{\mathrm{J}_1(\gamma)}{(\varepsilon_{on}^2 - \gamma^2)} \bar{D}_o + \frac{S\mathrm{J}_o(\varepsilon_{on})}{D^* \varepsilon_{mn}(\varepsilon_{on}^4 - \gamma^4)} \tilde{A}_{on} + \frac{\mathrm{J}_o(\varepsilon_{on})}{S}\left[\tilde{B}_{on} + \frac{\varepsilon_{on}}{\sqrt{\varepsilon_{on}^2 + S}} \tilde{D}_{on}\right] = 0 \tag{51b}$$

for $n = 1, 2, \ldots$ Here the previous expansion for $\mathrm{I}_o\left(\gamma \frac{r}{a}\right)$ and the equation

$$\mathrm{J}_o\left(\gamma \frac{r}{a}\right) = \frac{2}{\gamma} \mathrm{J}_1(\gamma) + 2\gamma \sum_{n=1}^{\infty} \frac{\mathrm{J}_1(\gamma)\mathrm{J}_o(\varepsilon_{on}\, r/a)}{\mathrm{J}_o(\varepsilon_{on})(\varepsilon_{on}^2 - \gamma^2)}$$

have been employed. In equations (51a, b), (50a, b), (42), (43), (41), equation (38) for $m = 0$ with the additional term $\bar{P}_o$, and (36) represent $(4n + 5)$ linear homogeneous equations in the constant $\tilde{A}_{on}$, $\tilde{B}_{on}$, $\tilde{C}_{on}$, $\tilde{D}_{on}$ and $\bar{A}_o$, $\bar{C}_o$, $\bar{D}_o$, P_o^* and $\bar{P}_o$, of which the vanishing coefficient determinant is the coupled frequency equation for axisymmetric motion.

4. NUMERICAL EVALUATIONS AND DISCUSSIONS

Some of the above-obtained analytical results have been evaluated numerically. For reasons of space, we have concentrated only on a limited amount of results with a membrane as a structural member, where some coupled axisymmetric ($m = 0$) and asymmetric ($m = 1, 2$) oscillations have been investigated. The basic parameters of the present coupled liquid–membrane system are given as: tension parameter $T^* \equiv Ta/\rho v^2$, surface tension parameter $\sigma^* \equiv \sigma a/\rho v^2 = (Oh)^{-2}$, gravitational parameter $g^* \equiv ga^3/v^2 = Bo/(Oh)^2$, membrane mass parameter $\mu^* \equiv \mu/\rho a$, the liquid height ratio h/a, the angular vibration mode m and radial vibration mode n. The above solution is in particular important for small liquid height ratios h/a, for which most of the liquid participates in the motion, and for which the adhesive effect of the container bottom contributes the major part to the damped motion. This is due to the fact that the wave motion penetrates to only about a depth of the order of one wavelength. Therefore the coupling of the liquid–structure system shows for small h/a a strong effect on the frequencies. For this reason, the range of the liquid height ratio was chosen to be $0 \leqslant h/a \leqslant 0{\cdot}5$. For a stiffer bottom, the interaction will become less pronounced due to the spread of the liquid and membrane frequencies involved. For large liquid height ratios h/a, the lower part of the liquid nearly behaves like a rigid body, while sloshing takes place in the immediate vicinity of the free liquid surface, indicating that the sloshing motion and membrane oscillations hardly influence each other. Therefore the influence of the adhesive bottom condition upon the damping diminishes, which suggests that for such a case the adhesive conditions at the wall, i.e., $v = w = 0$ at $r = a$ (which are neglected in the above analysis) will have paramount influence on the damping behavior of the liquid. Such a case will require a different analytical approach for the solution of the problem, which shall be the subject of a follow-on investigation.

In previous investigations [31, 32], for a rigid container bottom the results show for small liquid height ratios h/a, that the viscous liquid is no longer able to perform a damped oscillatory motion, but exhibits only an aperiodic behavior, if disturbed. This newly detected phenomenon has been obtained for a certain small range of h/a, depending on some system parameters. In the mentioned investigation, the decrease of the surface tension parameter $\sigma^* \equiv \sigma a/\rho v^2$ increases this aperiodic region. In addition, with increasing gravity parameter $g^* \equiv ga^3/v^2$ the aperiodic region decreases, while the domain, in which oscillations of the liquid appear, exhibits increased magnitude of the decay- and oscillation frequency. The viscous oscillation frequency increases for increasing liquid height ratio h/a, while the decay magnitude decreases. This means that for a larger liquid height ratio h/a, the damped liquid motion exhibits a less strong decay at larger oscillation frequency. This was found valid for slipping as well as for anchored contact line, except that the latter case shows both increased decay and oscillation frequency. The increase of the surface tension parameter increases the oscillation frequency of the liquid. Thus increasing height ratio h/a diminishes the influence of the container bottom effect upon the motion.

In the numerical evaluation of the above-presented analysis, we shall distinguish and evaluate two cases:

1. frictionless liquid, and
2. viscous liquid

and compare the coupled frequencies of the liquid and that of the membrane with their uncoupled values (rigid case), i.e., (natural frequencies). For a rigid container bottom, i.e., no elastic interaction with the bottom structure, we obtain the natural liquid frequencies, of which the anchored ones exhibit always larger magnitude than those for a slipping contact line. Such results would also appear if elastic interaction with the container bottom would be allowed. Such results are omitted here and only the case of an anchored contact line is numerically treated.

The membrane exhibits, without an additional liquid mass attached to it, the natural frequencies

$$\omega_{mn}^{(m)} = \frac{\bar{\varepsilon}_{mn}}{a}\sqrt{\frac{T}{\mu}} \quad \text{or} \quad \frac{\omega_{mn}^{(m)} a^2}{v} = \bar{\varepsilon}_{mn}\sqrt{\frac{T^*}{\mu^*}}, \tag{52}$$

where $\bar{\varepsilon}_{mn}$ are the roots of $J_m(\bar{\varepsilon}) = 0$, i.e. $\bar{\varepsilon}_{on} = 2{\cdot}405,\ 5{\cdot}520,\ 8{\cdot}654 \cdots$ and $\bar{\varepsilon}_{1n} = 3{\cdot}832,\ 7{\cdot}016,\ 10{\cdot}173 \cdots$. With the additional (non-sloshing) liquid mass on the membrane, the uncoupled (natural) frequencies would be

$$\frac{\omega_{mn}^{(m)} a^2}{v} = \bar{\varepsilon}_{mn}\sqrt{\frac{T^*}{\mu^* + h/a}} \tag{53}$$

indicating a decrease of the frequency as the liquid mass, i.e., the liquid height ratio h/a increases. The uncoupled sloshing frequencies are given by [36]

$$\omega_{mn}^{(s)^2} = \left[\frac{\varepsilon_{mn} g}{a} + \frac{\sigma \varepsilon_{mn}^3}{\rho a^3}\right] \tanh\left(\varepsilon_{mn}\frac{h}{a}\right),$$

where ε_{mn} are the roots of $J'_m(\varepsilon) = 0$. This may be expressed as

$$\frac{\omega_{mn}^{(s)} a^2}{v} = \left[\varepsilon_{mn}\left(g^* + \sigma^* \varepsilon_{mn}^2\right) \tanh\left(\varepsilon_{mn}\frac{h}{a}\right)\right]^{1/2}. \tag{54}$$

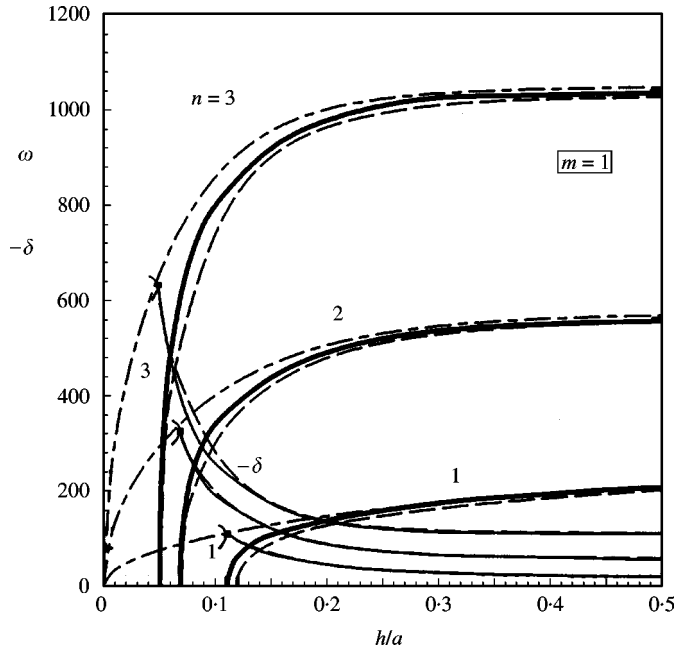

Figure 2. Coupled complex and uncoupled non-viscous frequencies of asymmetric motion $m = 1$; $T^* = 10^4$, $g^* = 10^4$, $\mu^* = 10^{-2}$ and $\sigma^* = 10^3$; uncoupled non-viscous frequencies (- · – · – · – · -), viscous liquid frequencies in container with rigid bottom (- – – – –), coupled complex frequencies for viscous liquid (——).

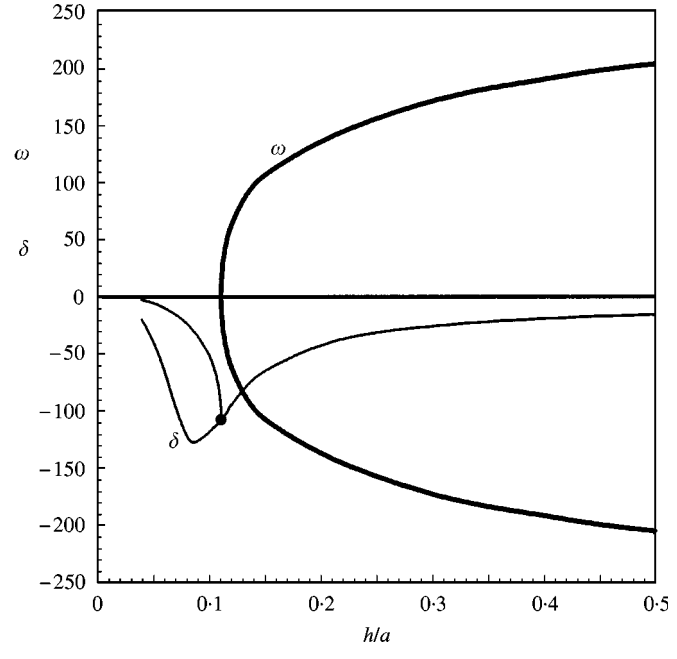

Figure 3. Coupled complex frequency for mode $m = 1$; $n = 1$; $T^* = 10^4$, $g^* = 10^4$, $\mu^* = 10^{-2}$ and $\sigma^* = 10^3$.

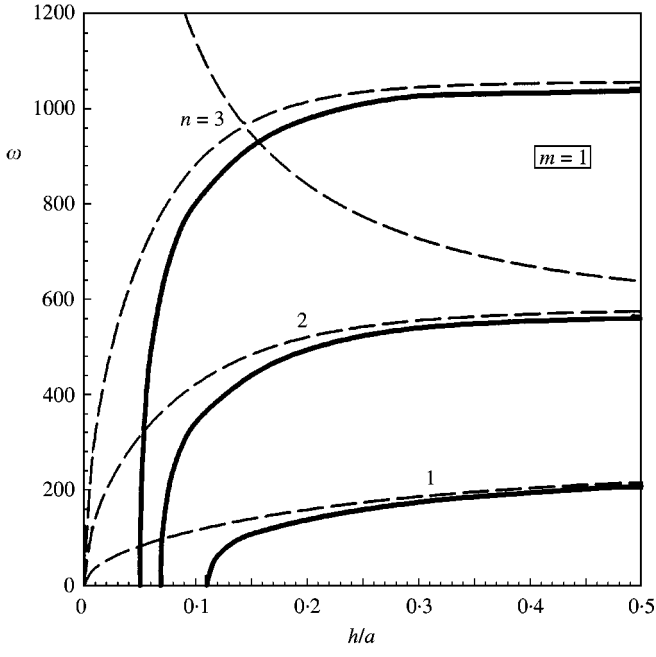

Figure 4. Coupled viscous and non-viscous frequencies for asymmetric motion mode $m = 1$; $T^* = 10^4$, $g^* = 10^4$, $\mu^* = 10^{-2}$ and $\sigma^* = 10^3$; viscous (——), non-viscous (- - - - -).

We restrict our numerical evaluations to the parameters magnitudes $T^* = 10^4, g^* = 10^4$, $\sigma^* = 10^3$ and $\mu^* = 10^{-2}$ and investigate the influence of the liquid height ratio h/a and angular- as well as radial mode number m and n respectively. For comparison, we use the uncoupled and coupled [37] frequencies of frictionless liquid and the complex frequencies of viscous liquid in a container with a rigid bottom [31, 32].

In Figure 2, the coupled complex asymmetric frequencies ($m = 1$) of the viscous liquid are presented and compared with the complex frequencies of the viscous liquid in a container with a rigid bottom. In addition, the natural frequencies of a frictionless liquid (–·–·–·–) are shown. The solid lines are the coupled damped frequencies and their decay magnitudes. First of all, we notice that the coupled damped frequency increases with increasing liquid height ratio h/a, and that the decay magnitude decreases. This means that at a larger liquid height ratio, the coupled motion of the liquid is represented by a less decaying oscillation of higher frequency. In addition, we detect that below $h/a = 0{\cdot}111$ only an aperiodic motion may appear for the first radial mode $n = 1$. For the liquid in a container with a rigid bottom, the oscillation frequency is lower than that of the liquid in a container with an elastic membrane bottom. The range of aperiodic motion is in a rigid bottom case slightly enlarged and exhibits the value of $0 \leqslant h/a \leqslant 0{\cdot}119$. This shows that the flexibility of the bottom allows the liquid to continue oscillating in a smaller height range h/a, thus enhancing oscillations. The natural frequencies for frictionless liquid are always larger. We notice also that the decay magnitude is slightly increased for the liquid in the container with a rigid bottom, indicating slightly larger decreases in higher modes n and smaller liquid height ranges h/a. The heavily indicated point on the δ-curves represents the double root, below which only aperiodic motion is possible. This is for the radial modes $n = 2$ and 3, the ranges $0 \leqslant h/a \leqslant 0{\cdot}069$ and $0 \leqslant h/a \leqslant 0{\cdot}050$ respectively. The two aperiodic branches are not presented, but only indicated in the graphs. In Figure 3, we just represent the mode $m = n = 1$ for a clearer interpretation of the facts just mentioned. The results of

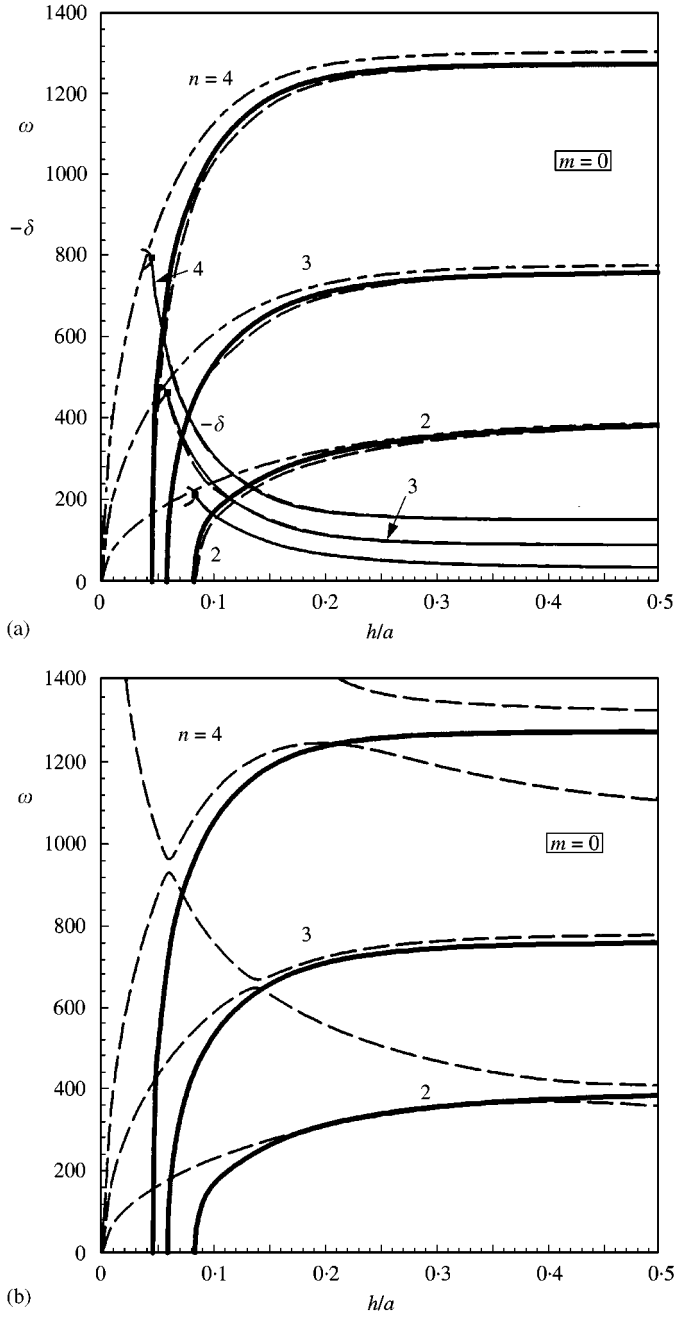

Figure 5. (a) Coupled complex and uncoupled non-viscous axisymmetric frequencies $m = 0$; $T^* = 10^4$, $g^* = 10^4$, $\mu^* = 10^{-2}$ and $\sigma^* = 10^3$; uncoupled non-viscous frequencies (-·-·-·-·-), viscous liquid frequencies with rigid bottom (- - - - -), coupled complex frequencies (▬▬). (b) Coupled viscous and non-viscous frequencies for axisymmetric motion $m = 0$; $T^* = 10^4$, $g^* = 10^4$, $\mu^* = 10^{-2}$ and $\sigma^* = 10^3$; viscous (▬▬), non-viscous (- - - - -).

Figures 2 and 3 have all been compared with those of the viscous liquid frequencies in a container with a rigid bottom. It was found that the results of Figure 2 agree very well with previous results and those in the case of an elastic membrane bottom for $h/a = 0{\cdot}5$. The

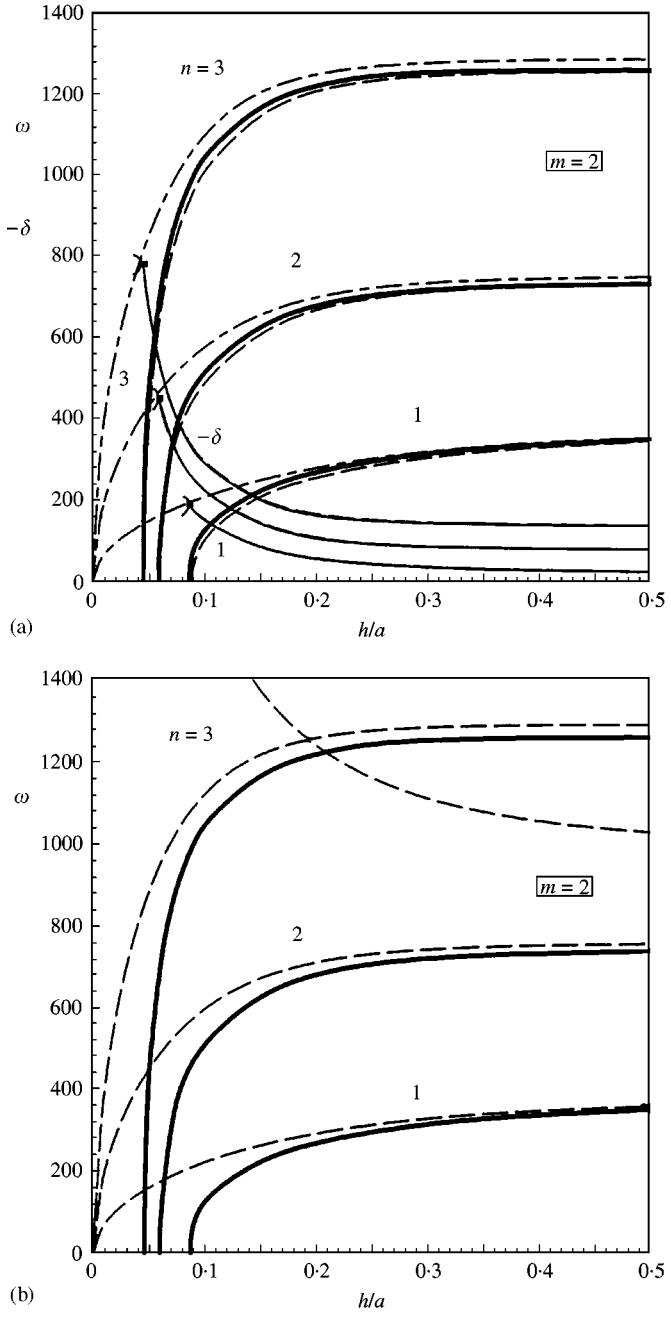

Figure 6. (a) Coupled complex and uncoupled non-viscous frequencies for mode $m = 2$; $T^* = 10^4$, $g^* = 10^4$, $\mu^* = 10^{-2}$ and $\sigma^* = 10^3$; uncoupled non-viscous frequencies (-·-·-·-·-), viscous liquid frequencies with rigid bottom (- - - - -), coupled complex frequencies (——). (b) Coupled viscous and non-viscous frequencies for $m = 2$; $T^* = 10^4$, $g^* = 10^4$, $\mu^* = 10^{-2}$ and $\sigma^* = 10^3$; viscous (——), non-viscous (- - - - -).

damped oscillation frequency of about $\omega \approx 205$ is larger than that of the rigid bottom case [31], which exhibits a magnitude of $\omega_{rigid} \approx 199$. The same is true for the decay magnitude which is $\delta \approx -15{\cdot}7$ and $\delta_{rigid} \approx -15{\cdot}9$, indicating that the liquid in a container with an elastic bottom decays less fast and for that reason oscillates much longer.

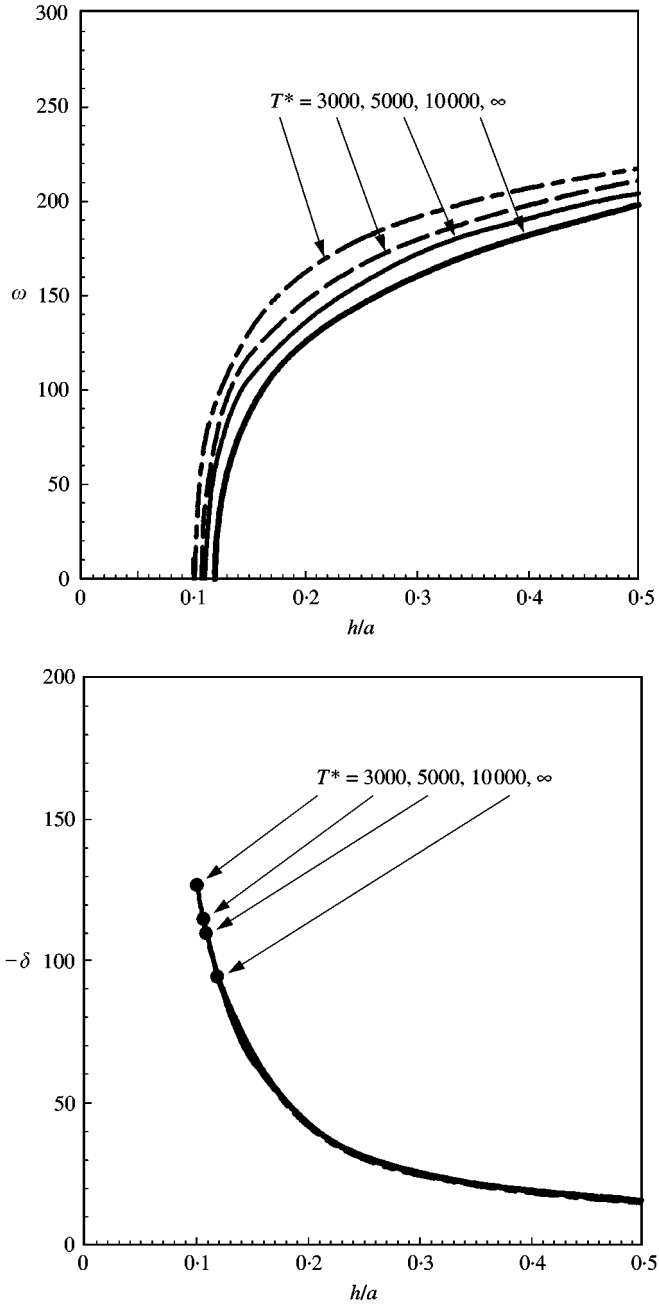

Figure 7. Effect of membrane tension T^* on coupled complex liquid frequency for mode $m = 1$, $n = 1$; $g^* = 10^4$, $\mu^* = 10^{-2}$ and $\sigma^* = 10^3$: $T^* = \infty$, 10^4, 5×10^3, 3×10^3.

In Figure 4, we represent just the oscillation frequencies ω, where we notice the strong decrease of the coupled membrane frequency [37] with the increase of the liquid height ratio h/a. This effect is due to the growing liquid mass added to the membrane with the growth of the liquid depth.

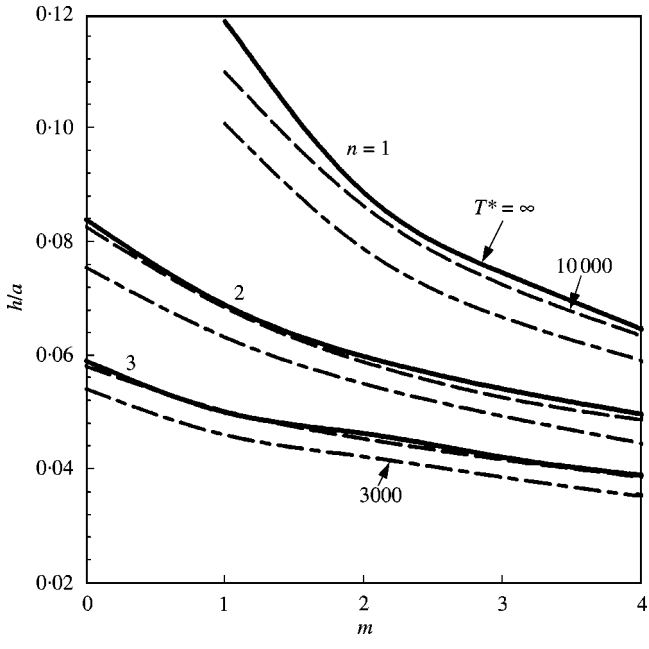

Figure 8. Effect of membrane tension T^* on critical liquid height, below which only aperiodic motion is possible: $m = 0, 1, 2, 3, 4$, $n = 1, 2, 3$; $g^* = 10^4$, $\mu^* = 10^{-2}$ and $\sigma^* = 10^3$. $T^* = \infty, 10^4, 3 \times 10^3$.

In Figure 5(a), the coupled axisymmetric complex frequencies $m = 0$ are presented together with those for a rigid bottom and the frictionless uncoupled frequencies (natural frequencies). We notice again the growth of the oscillation frequencies with increasing liquid height ratio h/a and in addition the range of aperiodicity. We also detect the decrease of the decay magnitude as h/a increases. In Figure 5(b), we represent just oscillation frequencies ω as in Figure 4.

Similar results are presented for the mode $m = 2$ (Figure 6(a) and 6(b)) which show similar effects. For all cases $m = 0, 1, 2$, the range of aperiodicity may be seen in Figure 8. In Figure 7, we represent the effect of the membrane tension T^* on the magnitude of the decay δ and the oscillation frequency ω, by changing the tension parameter $T^* \equiv Ta/\rho v^2$ as indicated from 3×10^3 to infinity.

First of all, we detect that the decay magnitude does not change much as T^* increases. We only notice that for smaller T^*-values the magnitude δ is slightly smaller. This is presented in this figure for the lowest vibration mode $m = n = 1$. The points in the δ-graph indicate the beginning of the aperiodic motion range for this mode and exhibit with increasing flexibility of the membrane, i.e., decreasing T^*, a decrease of that aperiodic range. For increasing T^* the oscillation frequency ω decreases as indicated in the ω-graph. This shows that the deviation due to increase of the tension parameter is quite visible for the oscillation frequency ω, but has a minor influence upon the decay magnitude. In Figure 8, we have determined the critical point for the various angular modes m and radial modes n, below which the liquid shall only perform an aperiodic motion. The influence of the membrane tension parameter T^* is shown to be decreasing the aperiodic range with decreasing T^* for all modes indicated. We also notice that for $m = 0$ the mode $n = 1$ does not exist.

In Figure 9(a) and 9(b), we exhibit the free liquid surface ζ and the membrane displacement ζ^* for the axisymmetric mode $m = 0$. In Figure 9(a), the membrane tension

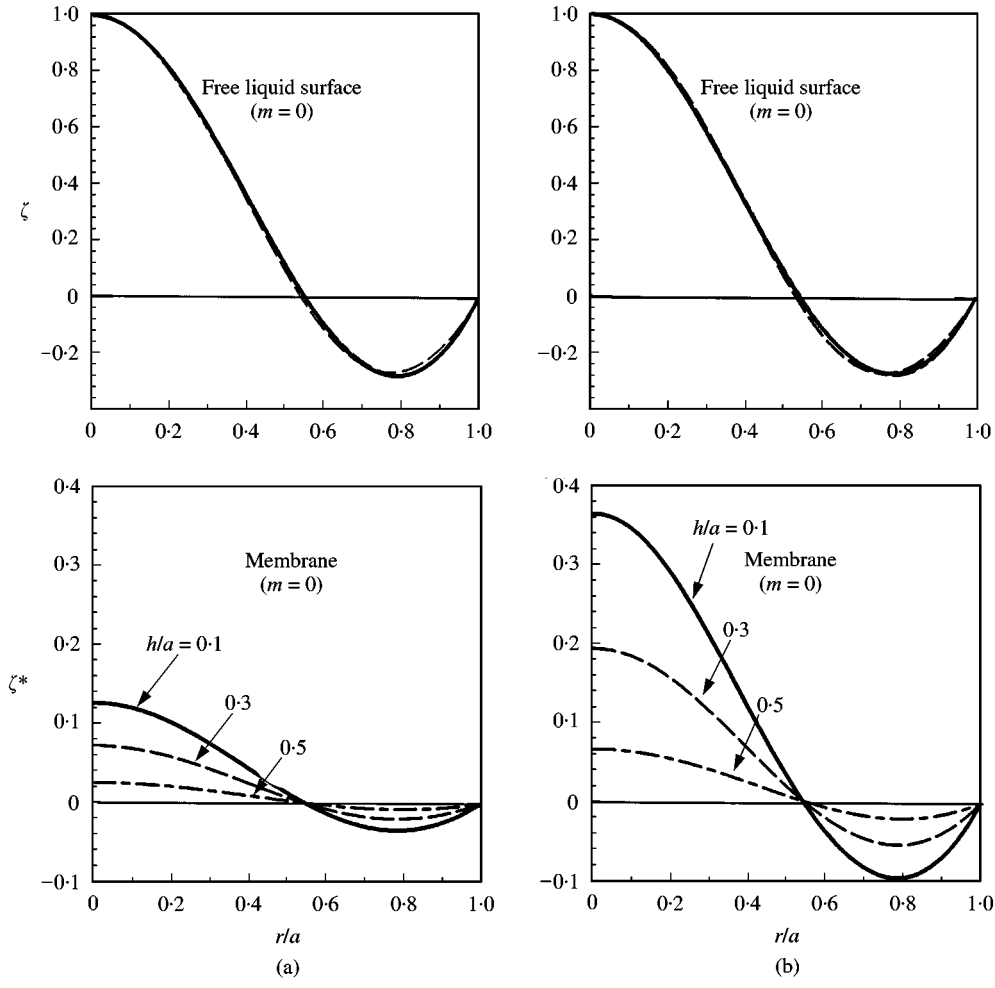

Figure 9. Vibration modes of the liquid free surface and membrane bottom for $m = 0$, $n = 1$; $g^* = 10^4$, $\mu^* = 10^{-2}$ and $\sigma^* = 10^3$: $h/a = 0{\cdot}1$, $0{\cdot}3$, $0{\cdot}5$; (a) $T^* = 10^4$; (b) $T^* = 3 \times 10^3$.

parameter was chosen to be $T^* = 10^4$ and the liquid- and membrane displacement are presented for the three liquid fillings $h/a = 0{\cdot}1$, $0{\cdot}3$ and $0{\cdot}5$. In this case, the free liquid surface ζ and the membrane displacement ζ^* are normalized so that the maximum value is unity. The mode shape of the elevation of the free surface ζ is not much affected by the different fillings, while the membrane displacement ζ^* definitely shows strong increase for smaller liquid filling height h/a. Figure 9(b) exhibits similar results for a low membrane tension parameter of $T^* = 3 \times 10^3$. Also, it shows even larger membrane displacements, indicating that the more flexible the membrane is, the larger are its displacements; and the larger the filling heights, the less the displacements. Figure 10 exhibits such results for the asymmetric oscillation $m = 1$, where the free surface elevation exhibits only minor change for different liquid fillings and the membrane deflection shows again large deviations. Figure 11 presents the influence of the membrane tension parameter at the filling rate $h/a = 0{\cdot}3$. With the increase of T^* from 3×10^3 to 10^4, the maximum of the mode shape of the free liquid surface ζ shifts toward the inside

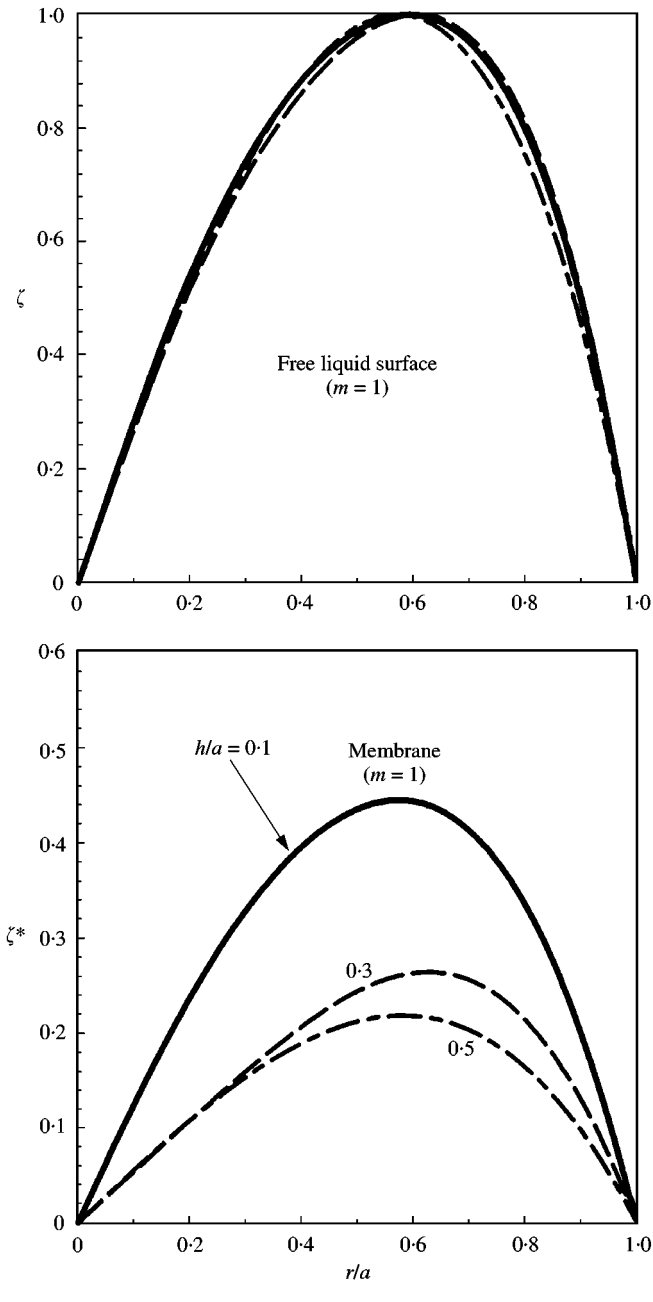

Figure 10. Vibration modes $m = 1$, $n = 1$; $T^* = 3 \times 10^3$, $g^* = 10^4$, $\mu^* = 10^{-2}$ and $\sigma^* = 10^3$: for different liquid height ratios $h/a = 0{\cdot}1$, $0{\cdot}3$, $0{\cdot}5$.

of the container, i.e., smaller r/a-values, while for the rigid bottom case ($T^* \to \infty$) the peak value shifts again towards the container wall. The deflection ζ^* of the membrane mode exhibits with increasing T^*-values a slight shift to the center of the membrane. In addition, the maximum of the mode shape decreases to zero as $T^* \to \infty$ (rigid bottom).

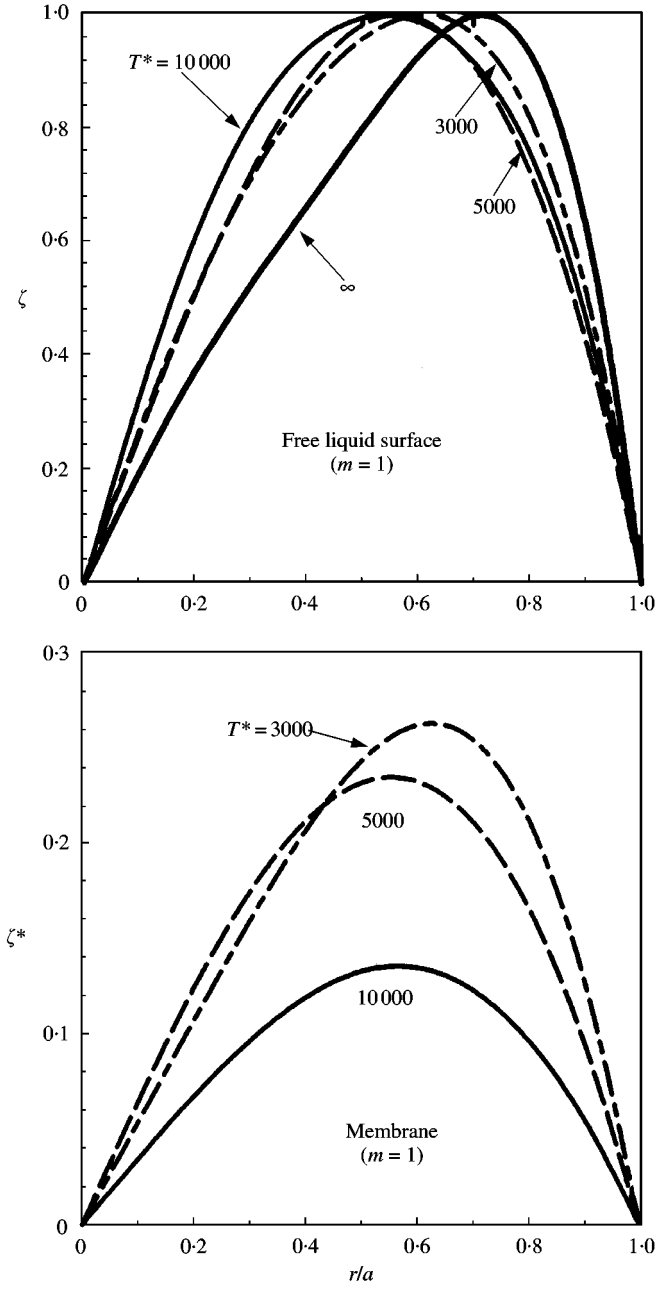

Figure 11. Effect of membrane tension T^* on vibration modes for $m = 1$; $n = 1$; $g^* = 10^4$, $\mu^* = 10^{-2}$, $\sigma^* = 10^3$ and $h/a = 0{\cdot}3$; $T^* = \infty$, 10^4, 5×10^3, 3×10^3.

5. CONCLUSIONS

From the above results we may conclude the following.

1. Viscosity introduces an aperiodic motion range for the lower liquid fillings.
2. With the growth of the mode number, the magnitude of the aperiodic range decreases.

3. With increasing liquid filling height, the decay magnitude decreases, while the oscillation frequency increases.
4. For higher modes, the oscillation frequencies exhibit larger values as do the decay magnitudes, indicating that higher modes are damped out rapidly.
5. Increase of the membrane tension T^* increases the aperiodic range, decreases the coupled liquid frequency, and has hardly any influence on the decay behavior.
6. Liquid filling ratio h/a has no effect upon the shape of the free liquid surface mode, but has a strong influence upon the mode shape of the membrane.
7. The growth of the filling rate decreases the magnitude of the membrane mode, while for decreased membrane tension parameter T^* the magnitude of the mode shape of the membrane is quite increased.

For the elastic bottom treated as a plate, the above procedure will be algebraically and numerically more complicated.

REFERENCES

1. J. W. MILES 1958 *Journal of Applied Mechanics* E **25**, 277–283. On the sloshing of liquid in a flexible tank.
2. U. S. LINDHOLM, D. D. KANA and H. N. ABRAMSON 1962 *Journal of Aerospace Sciences* **29**, 1052–1059. Breathing vibrations of a circular cylindrical shell with an internal liquid.
3. M. L. BARON and R. SKALAK 1962 *Proceedings of the American Society of Civil Engineers* **88**, 17–43. Free vibrations of fluid-filled cylindrical shells.
4. W.-H. CHU 1963 *Journal of Applied Mechanics* E **30**, 532–536. Breathing vibrations of a partially filled cylinder tank-linear theory.
5. P. G. BHUTA, G. PRAVIN and L. R. KOVAL 1964 *Zeitschrift für Angewandte Mathematik und Physik* **15**, 466–480. Coupled oscillations of a liquid with a free surface in a tank.
6. P. G. BHUTA and L. R. KOVAL 1964 *Journal of the Acoustical Society of America* **36**, 2071–2079. Hydroelastic solution of the sloshing of a liquid in a cylindrical tank.
7. E. SALEME and T. LIBER 1965 *Journal of the American Institute of Aeronautics and Astronautics* **3**, 132–136. Breathing vibrations of pressurized partially filled tanks.
8. H. F. BAUER, J. SIEKMANN and J. T. S. WANG 1968 *Journal of Spacecraft and Rockets* **5**, 981–983. Axisymmetric hydroelastic sloshing in an annular cylindrical container.
9. H. F. BAUER, T.-H. HSU and J. T. S. WANG 1968 *American Society of Mechanical Engineers Journal of Basic Engineering* **90**, 373–377. Interaction of a sloshing liquid with elastic containers.
10. T. Y. TSUI and N. C. SMALL 1968 *Journal of Spacecraft and Rockets* **5**, 202–206. Hydroelastic oscillations of a liquid surface in an annular circular cylindrical tank with flexible bottom.
11. H. F. BAUER and J. SIEKMANN 1969 *Zeitschrift für Angewandte Mathematik und Mechanik* **49**, 577–589. Note on linear hydroelastic sloshing.
12. A. W. LEISSA 1969 *NASA-SP*-160. *Washington, D.C.* Vibration of Plates.
13. H. F. BAUER 1970 *Zeitschrift für Flugwissenschaften* **18**, 117–134. Hydroelastische Schwingungen im aufrechten Kreiszylinderbehälter.
14. H. F BAUER and J. SIEKMANN 1971 *Ingenieur Archiv* **40**, 266–280. Dynamic interaction of a liquid with the elastic structure of a circular cylindrical container.
15. H. F. BAUER, J. T. S. WANG and P. Y. CHEN 1972 *Aeronautical Journal* **76**, 704–712. Axisymmetric hydroelastic sloshing in a circular cylindrical container.
16. H. F. BAUER 1973 *Zeitschrift für Flugwissenschaften* **21**, 202–213. Hydroelastische Schwingungen im einem starren Kreiszylinder bei elastischer Flüssigkeitsoberflächenabdeckung.
17. W. E. STILLMAN 1973 *Journal of Sound and Vibration* **30**, 509–524. Free vibration of cylinders containing liquid.
18. R. K. JAIN 1974 *Journal of Sound and Vibration* **37**, 379–388. Vibration of fluid-filled, orthotropic cylindrical shells.
19. W. A. NASH, S. H. SHAABAN and T. MONZAKIS 1980 *Proceedings of the* 3*rd IUTAM Symposium on Shell Theory*, 393–403. Amsterdam: North-Holland. Response of liquid storage tanks to seismic motion.

20. M. A. HAROUN and G. W. HOUSNER 1981 *Journal of Applied Mechanics* E **48**, 411–418. Earthquake response of deformable liquid storage tanks.
21. T. ANG, BALENDRA, P. K. K. PARAMASIVAM and S. L. LEE 1982 *International Journal of Mechanical Science* **24**, 47–59. Free vibration analysis of cylindrical liquid storage tanks.
22. N. YAMAKI, J. TANI and T. YAMAJI 1984 *Journal of Sound and Vibration* **94**, 531–550. Free vibration of a clamped–clamped circular cylindrical shell partially filled with liquid.
23. M. CHIBA 1993 *Journal of Fluids and Structures* **7**, 57–73. Non-linear hydroelastic vibration of a liquid-contained cylindrical tank with an elastic bottom, part II: Linear axisymmetric vibration analysis.
24. M. CHIBA 1996 *International Journal of Non-linear Mechanics* **31**, 155–165. Non-linear hydroelastic vibration of a cylindrical tank with an elastic bottom containing liquid-III. Non-linear analysis with Ritz averaging method.
25. M. CHIBA 1997 *Journal of Sound and Vibration* **202**, 417–426. The influence of elastic bottom plate motion on the resonant response of a liquid free surface in a cylindrical container: a linear analysis.
26. M. CHIBA and K. ABE 1999 *Thin-Walled Structures* **34**, 233–260. Nonlinear hydroelastic vibration of a cylindrical tank with an elastic bottom containing liquid-analysis using Harmonic Balance method.
27. D. M. HENDERSON and J. W. MILES 1994 *Journal of Fluid Mechanics* **275**, 285–299. Surface-wave damping in a circular cylinder with a fixed contact line.
28. C. MARTEL, J. A. NICOLAS and J. M. VEGA 1988 *Journal of Fluid Mechanics* **360**, 213–228. Surface-wave damping in a brimful circular cylinder.
29. J. M. MILES and D. M. HENDERSON 1998 *Journal of Fluid Mechanics* **364**, 319–323. A note on interior vs. boundary-layer damping of surface waves in a circular cylinder.
30. K. H. CASE and W. C. PARKINSON 1957 *Journal of Fluid Mechanics* **2**, 172–184. Damping of surface waves in an incompressible liquid.
31. H. F. BAUER and W. EIDEL 1997 *Forschung im Ingenieurwesen – Engineering Research* **63**, 189–201. Axisymmetric viscous liquid oscillations in a cylindrical container.
32. H. F. BAUER and W. EIDEL 1997 *Aerospace Science and Technology* **8**, 519–532. Oscillations of a viscous liquid in a cylindrical container.
33. H. F. BAUER and W. EIDEL 1999 *Forschung im Ingenieurwesen – Engineering Research* **65**, 191–199. Axisymmetric natural damped frequencies of a viscous liquid in a circular cylindrical container. – An alternative semi-analytical solution.
34. H. F. BAUER and W. EIDEL 1999 *Aerospace Science and Technology* **8**, 495–512. Free oscillations and response of a viscous liquid in a circular cylindrical tank.
35. H. F. BAUER and M. CHIBA 2000 *Journal of Fluids and Structures*. **14**, 917–936. Hydroelastic viscous oscillations in a circular cylindrical container with an elastic cover.
36. H. F. BAUER 1964 NASA-TR-R-187. Fluid oscillations in the container of a space vehicle and their influence upon stability.
37. M. CHIBA, H. WATANABE and H. F. BAUER Hydroelastic coupled vibrations in a cylindrical container with a membrane bottom, containing liquid with surface tension. (to appear)
38. G. N. WATSON 1966 A Treatise on the Theory of Bessel Function. Cambridge: Cambridge University Press.

APPENDIX A: NOMENCLATURE

a	radius of cylindrical container
Bo	Bond number ($Bo \equiv \rho g a^2/\sigma$)
D	flexural rigidity of the elastic plate ($D^* \equiv D/\rho v^2 a$)
E	Young's modulus of elasticity
g	gravitational acceleration ($g^* \equiv g a^3/v^2$)
h	liquid height
I_m	modified Bessel function of order m and first kind
i	imaginary unit
J_m	Bessel function of order m and first kind
M_r	moment
Oh	Ohnesorge number $\equiv (\sigma^*)^{-1/2}$
p	liquid pressure

p_o	static pressure
r, φ, z	polar coordinate system
S	$\equiv sa^2/\nu (s = \bar{\sigma} + \mathrm{i}\bar{\omega}$ complex frequency)
T	tension of membrane ($T^* \equiv Ta/\rho\nu^2$)
t	time ($\tau \equiv t\nu/a^2$)
u, v, w	velocity components of liquid
V_r	shear force
α	parameter $\alpha^2 \equiv \dfrac{\rho g a^2}{\sigma} \equiv \dfrac{g^*}{\sigma^*} = Bo$
β	parameter $\beta^2 \equiv (\mu^* S^2 + g^*)/T^*$
β^{*4}	$(\mu^* S^2 + g^*)/D^*$
γ	parameter defined by $\gamma \equiv \sqrt{\mathrm{i}}\beta^*$
δ	$\equiv \bar{\sigma} a^2/\nu$ dimensionless decay magnitude
δ^*	plate thickness
ε_{mn}	roots of $\mathrm{J}'_m(\varepsilon) = 0$
$\bar{\varepsilon}_{mn}$	roots of $\mathrm{J}_m(\bar{\varepsilon}) = 0$
η	dynamic viscosity
$\bar{\mu}_{mn}$	parameter defined by $\bar{\mu}^2_{mn} \equiv \varepsilon^2_{mn} + S$
μ	mass per unit area of membrane or plate ($\mu^* \equiv \mu/\rho a$)
ν	$\equiv \eta/\rho$ kinematic viscosity
$\bar{\nu}$	Poisson's ratio of plate
ξ^*, η^*, ζ^*	displacement of membrane or plate
ζ	free surface displacement
ρ	mass density of liquid
σ	surface tension of liquid ($\sigma^* \equiv \sigma a/\rho\nu^2$)
ϕ, ψ	defined by equation (17a)
ω	$\equiv \bar{\omega} a^2/\nu$ dimensionless oscillation frequency
$\omega^{(m)}$	uncoupled natural frequency of membrane
$\omega^{(s)}$	uncoupled natural frequency of liquid